PCCP

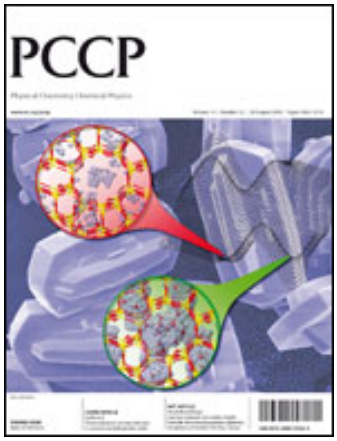

Physical Chemistry Chemical Physics

This paper is published as part of a PCCP Themed Issue on:

Water at interfaces

Guest Editor: Martin McCoustra

Editorial

Communications

Papers

Raman spectra of complexes of HNO_3 and NO_3^- with NO_2 at surfaces and with N_2O_4 in solution
Michael A. Kamboures, Wytze van der Veer, R. Benny Gerber and Leon F. Phillips, *Phys. Chem. Chem. Phys.*, 2008, **10**, 4748
DOI: 10.1039/b810081k

Molecular level structure of the liquid/liquid interface. Molecular dynamics simulation and ITIM analysis of the water-CCl_4 system
Lívia B. Pártay, George Horvai and Pál Jedlovszky, *Phys. Chem. Chem. Phys.*, 2008, **10**, 4754
DOI: 10.1039/b807299j

Solvent structures of mixed water/acetonitrile mixtures at chromatographic interfaces from computer simulations
Jörg Braun, Antony Fouqueau, Raymond J. Bemish and Markus Meuwly, *Phys. Chem. Chem. Phys.*, 2008, **10**, 4765
DOI: 10.1039/b807492e

Ion spatial distributions at the liquid–vapor interface of aqueous potassium fluoride solutions
Matthew A. Brown, Raffaella D'Auria, I.-F. William Kuo, Maria J. Krisch, David E. Starr, Hendrik Bluhm, Douglas J. Tobias and John C. Hemminger, *Phys. Chem. Chem. Phys.*, 2008, **10**, 4778
DOI: 10.1039/b807041e

Trapping proton transfer intermediates in the disordered hydrogen-bonded network of cryogenic hydrofluoric acid solutions
Patrick Ayotte, Sylvain Plessis and Patrick Marchand, *Phys. Chem. Chem. Phys.*, 2008, **10**, 4785
DOI: 10.1039/b806654j

Aqueous divalent metal–nitrate interactions: hydration *versus* ion pairing
Man Xu, James P. Larentzos, Mazen Roshdy, Louise J. Criscenti and Heather C. Allen, *Phys. Chem. Chem. Phys.*, 2008, **10**, 4793
DOI: 10.1039/b807090n

Structure and dynamics of water at a clay surface from molecular dynamics simulation
Virginie Marry, Benjamin Rotenberg and Pierre Turq, *Phys. Chem. Chem. Phys.*, 2008, **10**, 4802
DOI: 10.1039/b807288d

Proton mobility in thin ice films: a revisit
Eui-Seong Moon, Chang-Woo Lee and Heon Kang, *Phys. Chem. Chem. Phys.*, 2008, **10**, 4814
DOI: 10.1039/b807730b

Thermodynamics of water intrusion in nanoporous hydrophobic solids
Fabien Cailliez, Mickael Trzpit, Michel Soulard, Isabelle Demachy, Anne Boutin, Joël Patarin and Alain H. Fuchs, *Phys. Chem. Chem. Phys.*, 2008, **10**, 4817
DOI: 10.1039/b807471b

Gas phase hydration of organic ions
Paul O. Momoh and M. Samy El-Shall, *Phys. Chem. Chem. Phys.*, 2008, **10**, 4827
DOI: 10.1039/b809440n

Water photodissociation in free ice nanoparticles at 243 nm and 193 nm
Viktoriya Poterya, Michal Fárník, Milan Ončák and Petr Slavíček, *Phys. Chem. Chem. Phys.*, 2008, **10**, 4835
DOI: 10.1039/b806865h

Electroacoustic and ultrasonic attenuation measurements of droplet size and ζ-potential of alkane-in-water emulsions: effects of oil solubility and composition
Alex M. Djerdjev and James K. Beattie, *Phys. Chem. Chem. Phys.*, 2008, **10**, 4843
DOI: 10.1039/b807623e

Gas hydrate nucleation and cage formation at a water/methane interface
Robert W. Hawtin, David Quigley and P. Mark Rodger, *Phys. Chem. Chem. Phys.*, 2008, **10**, 4853
DOI: 10.1039/b807455k

Hydration water rotational motion as a source of configurational entropy driving protein dynamics. Crossovers at 150 and 220 K
J.-M. Zanotti, G. Gibrat and M.-C. Bellissent-Funel, *Phys. Chem. Chem. Phys.*, 2008, **10**, 4865
DOI: 10.1039/b808217k

Influence of wettability and surface charge on the interaction between an aqueous electrolyte solution and a solid surface
Svetlana Guriyanova and Elmar Bonaccurso, *Phys. Chem. Chem. Phys.*, 2008, **10**, 4871
DOI: 10.1039/b806236f

Molecular dynamics study of hydrated imogolite 2. Structure and dynamics of confined water
Benoît Creton, Daniel Bougeard, Konstantin S. Smirnov, Jean Guilment and Olivier Poncelet, *Phys. Chem. Chem. Phys.*, 2008, **10**, 4879
DOI: 10.1039/b803479f

Assessing the performance of implicit solvation models at a nucleic acid surface
Feng Dong, Jason A. Wagoner and Nathan A. Baker, *Phys. Chem. Chem. Phys.*, 2008, **10**, 4889
DOI: 10.1039/b807384h

Aqueous peptides as experimental models for hydration water dynamics near protein surfaces
Cecile Malardier-Jugroot, Margaret E. Johnson, Rajesh K. Murarka and Teresa Head-Gordon, *Phys. Chem. Chem. Phys.*, 2008, **10**, 4903
DOI: 10.1039/b806995f

Melting behavior of water in cylindrical pores: carbon nanotubes and silica glasses
M. Sliwinska-Bartkowiak, M. Jazdzewska, L. L. Huang and K. E. Gubbins, *Phys. Chem. Chem. Phys.*, 2008, **10**, 4909
DOI: 10.1039/b808246d

Increased interfacial thickness of the NaF, NaCl and NaBr salt aqueous solutions probed with non-resonant surface second harmonic generation (SHG)
Hong-tao Bian, Ran-ran Feng, Yan-yan Xu, Yuan Guo and Hong-fei Wang, *Phys. Chem. Chem. Phys.*, 2008, **10**, 4920
DOI: 10.1039/b806362a

Determination of the electron's solvation site on D_2O/Cu(111) using Xe overlayers and femtosecond photoelectron spectroscopy
Michael Meyer, Julia Stähler, Daniela O. Kusmierek, Martin Wolf and Uwe Bovensiepen, *Phys. Chem. Chem. Phys.*, 2008, **10**, 4932
DOI: 10.1039/b807314g

Breakdown of hydration repulsion between charged surfaces in aqueous Cs^+ solutions
Ronit Goldberg, Liraz Chai, Susan Perkin, Nir Kampf and Jacob Klein, *Phys. Chem. Chem. Phys.*, 2008, **10**, 4939
DOI: 10.1039/b807459n

A macroscopic water structure based model for describing charging phenomena at inert hydrophobic surfaces in aqueous electrolyte solutions
Johannes Lützenkirchen, Tajana Preočanin and Nikola Kallay, *Phys. Chem. Chem. Phys.*, 2008, **10**, 4946
DOI: 10.1039/b807395c

Thermally induced mixing of water dominated interstellar ices
Daren J. Burke, Angela J. Wolff, John L. Edridge and Wendy A. Brown, *Phys. Chem. Chem. Phys.*, 2008, **10**, 4956
DOI: 10.1039/b807220e

Water hydrogen bond analysis on hydrophilic and hydrophobic biomolecule sites
Daniela Russo, Jacques Ollivier and José Teixeira, *Phys. Chem. Chem. Phys.*, 2008, **10**, 4968
DOI: 10.1039/b807551b

Hydronium and hydroxide at the interface between water and hydrophobic media
Robert Vácha, Dominik Horinek, Max L. Berkowitz and Pavel Jungwirth, *Phys. Chem. Chem. Phys.*, 2008, **10**, 4975
DOI: 10.1039/b806432f

Average molecular orientations in the adsorbed water layers on silicon oxide in ambient conditions
Anna L. Barnette, David B. Asay and Seong H. Kim, *Phys. Chem. Chem. Phys.*, 2008, **10**, 4981
DOI: 10.1039/b810309g

Interfacial water structure at polymer gel/quartz interfaces investigated by sum frequency generation spectroscopy
Hidenori Noguchi, Minowa Hiroshi, Taiki Tominaga, Jian Ping Gong, Yoshihito Osada and Kohei Uosaki, *Phys. Chem. Chem. Phys.*, 2008, **10**, 4987
DOI: 10.1039/b807297n

Co-adsorption of water and hydrogen on Ni(111)
Junjun Shan, Jacques F. M. Aarts, Aart W. Kleyn and Ludo B. F. Juurlink, *Phys. Chem. Chem. Phys.*, 2008, **10**, 4994
DOI: 10.1039/b808219g

Water–methanol mixtures: topology of hydrogen bonded network
Imre Bakó, Tünde Megyes, Szabolcs Bálint, Tamás Grósz and Viorel Chihaia, *Phys. Chem. Chem. Phys.*, 2008, **10**, 5004
DOI: 10.1039/b808326f

Hydrophobic interactions between water and pre-adsorbed D on the stepped Pt(533) surface†

Maria J. T. C. van der Niet,* Isja Dominicus, Marc T. M. Koper and Ludo B. F. Juurlink

Received 6th June 2008, Accepted 16th September 2008
First published as an Advance Article on the web 20th October 2008
DOI: 10.1039/b809652j

We have studied the interaction of Pt(533) with varying coverages of water and varying coverages of pre-adsorbed deuterium (D_{ad}) under ultra-high vacuum conditions. We use temperature-programmed desorption and reflective absorption infrared spectroscopy techniques to study the properties of these layers. Results show that deuterium's preference to adsorb at step edges nulls the step-induced stabilization of water through an electronic effect. However, deuterium atoms at step edges do not block adsorption sites for water and water still wets the entire (111) terrace. With increasing deuterium coverage on terraces, formation of smaller, less-ordered water structures replaces formation of hexamer ring structures. Near deuterium saturation, water preferentially forms 3-dimensional amorphous solid water (ASW) clusters at the steps. The typical phase transition of ASW to crystalline ice is observed in these clusters. Although exchange of D_{ad} with H_2O occurs both at steps and terraces and is dependent on both surface coverages, the preference of water molecules to cluster at the step sites on the hydrophobic, deuterium-saturated Pt(533) surface biases exchange toward steps.

I. Introduction

The interaction between water and platinum surfaces has been studied extensively, because of its importance in electrochemistry, fuel cell catalysis, heterogeneous catalysis and corrosion chemistry. Two extensive reviews have appeared that summarize the large body of knowledge on water–surface interactions that has been obtained using a variety of surfaces, co-adsorbates and employed techniques.[1,2]

Most studies investigating the platinum–water interaction have used the (111) surface as a model. Although this is the least complex system, ultra-high vacuum (UHV) studies already show significant complexity in adsorption and desorption phenomena.[3–5] However, a real catalytic surface contains additional low coordination or defect sites. These defect sites are often thought to be more active for catalytic reactions involving bond breaking and making. Although some experiments have focused on the influence of steps and defects that are naturally present on a Pt(111) crystal,[6,7] more insight results from studies employing a better-defined model, such as a regularly stepped surface.[8,9] Co-adsorption of water with hydrogen, which is of particular interest to understanding the chemistry occurring at the anode of low-temperature fuel cells and the reversible hydrogen electrode (RHE), has received even less attention so far.[1,2]

The general consensus is that on Pt(111) water adsorbs molecularly at all coverages and temperatures (<180 K). Hydrogen bonding between water molecules already occurs at low coverages, leading to the formation of hexagonal ring structures.[2] An extensive high-resolution electron energy loss spectroscopy (HREELS) study by Jacobi *et al.* shows distinct differences in the vibrational spectra for water monomer, bilayer and multilayer structures.[10]

Water dosed on Pt(111) at temperatures well below 135 K yields growth of amorphous solid water (ASW).[11] Temperature-programmed desorption (TPD) studies of ASW show two peaks. One peak at 171 K is associated with monolayer (ML) desorption. This peak shows the characteristics of zero-order desorption kinetics[12] and has been attributed to co-existence of a condensed phase and a 2-dimensional water–gas at sub-monolayer coverages.[11] A second peak, associated with desorption from multilayers, starts at 154 K and increases in temperature with coverage.[13] Multilayers have been shown to crystallize during the TPD ramp.[11,14]

Only a few studies have been performed on the interaction between H_2O and stepped platinum surfaces.[6–9] Scanning tunneling microscopy (STM) studies on an imperfect Pt(111) crystal show that water adsorbs preferentially on step sites, forming molecular chains.[6] TPD shows a stabilization of the water monolayer by the presence of step sites.[8,9] A two-peak structure is observed for a monolayer of H_2O desorbing from the stepped Pt(533) surface (Pt[4(111) × (100)]). At coverages below 0.13 ML a single peak is observed, which Grecea *et al.* reported to shift with coverage from 194 to 198 K.[9] This peak is associated with desorption from step sites. At higher coverages (above ~0.33 ML) a shoulder appears at 185 K, which is associated with desorption from terrace sites. The

Leiden Institute of Chemistry, University of Leiden, Einsteinweg 55, P.O. Box 9502, 2300 RA Leiden, The Netherlands.
E-mail: jvanderniet@chem.leidenuniv.nl

† This article was submitted as part of a Themed Issue on water at interfaces. Other papers on this topic can be found in issue 32 of vol. 10 (2008). This issue can be found from the *PCCP* homepage [http://www.rsc.org/pccp].

peak associated with desorption from the water multilayer appears at ~160 K.[9]

Molecular hydrogen adsorbs dissociatively on both Pt(111)[15–17] and stepped platinum surfaces.[15,18–23] Electron energy loss spectroscopy (EELS) studies in combination with density functional theory (DFT) calculations have shown that on Pt(111) an adsorbed hydrogen atom (H_{ad}) binds preferentially in the threefold hollow sites at all fractional surface coverages (θ).[16,17,24] However, the vibrational modes observed for $\theta \leq 0.75$ (31 and 68 meV)[16] are different from the ones observed at higher coverages (68, 113 and 153 meV).[17] The modes at low coverages are non-localized, whereas the modes at 68 and 113 meV for $\theta > 0.75$ can be ascribed to the asymmetric and symmetric stretch at the fcc site modified by anharmonic effects. Baró and Ibach[20] performed an EELS study on the stepped Pt(332) surface (Pt[6(111) × (111)]). They assigned the mode at 1129 cm^{-1} to H_{ad} located on a bridge site at the inner corner of the (111) step. However, Olsen *et al.*[25] questioned this assignment on the basis of DFT calculations on Pt(211) (Pt[3(111) × (100)]). Their calculations show that on the Pt(211) surface a deep global minimum for hydrogen adsorption is located at the bridge site on top of the step edge. A high barrier hinders motion from the lower terrace to the step edge.

Quasielastic helium-atom scattering (QHAS) measurements on H and D diffusion on Pt(111) indicate that hydrogen diffusion takes place *via* an isotropic single-jump mechanism. A slightly higher barrier for diffusion is found for D_{ad} compared to H_{ad}.[26] An experimental study on the influence of steps on the diffusion of hydrogen atoms on Pt(111) shows that, compared to the flat Pt(111) surface, both diffusion parallel and diffusion perpendicular to the steps is enhanced by the presence of step sites. For low step densities (miscut angle of 1 or 2° along the $[\bar{1}\bar{1}2]$ or $[11\bar{2}]$ direction) diffusion perpendicular to the steps is faster than parallel to the steps. However, for high step densities (miscut angle of 4° along $[\bar{1}\bar{1}2]$ direction) diffusion perpendicular to the step edges becomes inhibited and slower than on the flat surface.[27]

Recent TPD experiments of hydrogen desorbing from Pt(533) show two desorption features: a large feature below 360 K and a smaller feature at 380 K.[22] The high temperature feature is associated with recombinative desorption from step sites, whereas the lower temperature desorption feature is associated with recombinative desorption from terrace sites and possibly some remaining step sites. This indicates preferential adsorption of hydrogen on step sites. The entire surface is saturated at 0.9 ± 0.05 ML, whereas the high temperature feature saturates at 0.14 ± 0.02 ML, indicating that only half of the (100) step sites would be covered with H_{ad}.[22] However, recent experiments from our laboratory report a higher coverage on the step sites of the Pt(533) surface and indicate a non-linear dependence between the ratio H adsorbed on step sites : H adsorbed on terrace sites ($H_{step} : H_{terrace}$) and step density.[28] The calculations of Olsen *et al.*[25] find that filling the other half of the step sites with hydrogen is energetically more favorable than hydrogen adsorption on terrace sites, though it is 0.05 eV less favorable compared to the first half coverage of H_{ad} on step sites.

The co-adsorption of water and hydrogen is especially relevant for electrochemistry. Flash-temperature desorption studies on H_2O desorbing from a hydrogen-covered Pt(111) surface[12,29,30] generally show an increase in desorption temperature of the monolayer desorption peak. Different magnitudes for this shift have been reported, ranging from 2 to 10 K. The monolayer desorption peak saturates at lower coverage than on the bare surface, forcing H_2O molecules into the multilayer desorption peak. A more recent D_2O TPD study[31] involving D_{ad} and D_2O co-adsorption shows that a new peak develops at higher desorption temperatures at the expense of the D_2O desorption feature at 170 K. The desorption temperature of this feature goes through a maximum at 176 K as a function of D_2 pre-dose. However, at all deuterium pre-coverages the new feature appears at higher temperatures than for the bare surface. Interestingly, on Pt(100) the desorption temperature decreases on the hydrogen-covered surface compared to the bare surface.[32]

Isotope labeling studies show exchange between D_{ad} and H_2O co-adsorbed on Pt(111)[30] and Pt(100).[32] HREELS[29,30] and reflective absorption infrared spectroscopy (RAIRS)[33] studies on the co-adsorption of H_{ad} and H_2O show an additional vibrational feature at 1150 cm^{-1} at hydrogen coverages above ~15% after annealing above 150 K. The same feature has been observed on Pt(100).[32] Initially the HREELS data reported no isotopic shift in the 1150 cm^{-1} peak when H_{ad} was replaced with D_{ad} on Pt(111).[30] Later a disappearance of the peak was reported on Pt(110) when D_{ad} was used.[34] RAIRS studies reported an isotopic shift to 850 cm^{-1} when D_2O and D_{ad} were co-adsorbed on Pt(111).[33]

The nature of this vibrational feature, and consequently the adsorbed species, has remained elusive. Since the peak is similar to the umbrella mode of H_3O^+ in mineral acids, initially it was concluded that a hydronium species was formed, though it was remarked that this did not necessarily imply the transfer of a full electron.[30] Later Chen *et al.*[34] calculated gas-phase vibrational spectra of different water–hydronium complexes and compared them to HREELS spectra on (2 × 1)Pt(110). They found that the formation of H_3O^+ was endothermic and a $[(H_2O)_xH^+]$ complex was a more likely candidate, though the agreement between theory and experiment was not as good as the authors expected. Other species considered were the H_3O radical, a $H–OH_2$ complex and anionic complexes. Interestingly the 1150 cm^{-1} peak is also observed when H_2 and H_2O are co-adsorbed on the Cu(110) surface.[30] However, on Cu(110) no isotopic exchange is seen in the desorption spectra and the formation of an hydronium species was excluded on this surface.

On Pt(111) Lackey *et al.*[30] have observed an initial decrease of ~650 mV in the work function when both H_2O and H_2 are adsorbed. Upon annealing to the temperature where the H/H_2O species is formed, an additional decrease of ~100 mV in the work function is reported. It was concluded that the formed species is positively charged, even though the decrease in the work function is not as large as expected for the transfer of a full electron. The change in work function could also be caused by a dipole rearrangement in water ice.[35]

A recent surface-enhanced infrared absorption spectroscopy (SEIRAS) study of the interfacial water layer on polycrystalline platinum shows the adsorption features under electrochemical conditions (in H_2SO_4 or $HClO_4$ solutions).[36]

In the potential region where H_2 evolves the ν(OH) band is observed at 3550 cm^{-1}, whereas the δ(HOH) band is observed at 1613 cm^{-1}. Overpotential-deposited hydrogen (H_{opd}), *i.e.* H adsorbed on Pt below the reversible hydrogen potential (0 V), adsorbed on atop sites is seen at 2080 cm^{-1}. At slightly higher potentials, where underpotential-deposited hydrogen (H_{upd}), *i.e.* H adsorbed on Pt above the reversible hydrogen potential (0 V), is adsorbed on the surface, the ν(OH) and concomitant δ(HOH) band red-shift. H_{upd} is supposedly adsorbed in fcc sites. The calculated perpendicular vibrational stretching frequency is 1017 cm^{-1}.[37] This species is not observed in the experiments of Osawa *et al.*[36] The hydronium band at $\sim$1720 cm^{-1} is only observed in bulk-phase water.

There is no experimental data on the co-adsorption of H_2O and H_{ad} on a stepped surface. However, as noted earlier, in order to understand what is happening on a real catalyst it is vital to know the influence of step and defect sites on the structure and stability of water and the catalytic activity. Therefore, we use TPD and RAIRS in conjunction with isotope labeling to investigate the influence of pre-adsorbed hydrogen (deuterium) on co-adsorbed H_2O on the stepped Pt(533) surface in UHV.

II. Experimental

Experiments were performed in an UHV apparatus, described in detail elsewhere,[38,39] with a base pressure of 2×10^{-10} mbar during experiments. The Pt(533) crystal was cleaned by repeated cycles of Ar^+ (Messer, 5.0) bombardment (3–4 μA, 20 min), annealing between 850 and 1000 K in an oxygen atmosphere (2×10^{-8} mbar), and annealing at 1200 K. Low-energy electron diffraction (LEED) images taken after cleaning procedures confirm that the surface consists of four atom wide (111) terraces. Water from a Millipore Milli-Q gradient A10 system (18.2 MΩ cm resistance) was deaerated in a glass container by multiple freeze–pump–thaw cycles and then kept at a total pressure of 1.2 bar He (Linde gas, 5.0). The container was connected to a home-built glass capillary-array doser located in the infrared cell of the UHV apparatus. Water was dosed directly on the surface at a rate of $\sim$0.007 ML s^{-1} by measuring the pressure rise due to the co-dosed helium. Both H_2 (Linde gas, 5.0) and D_2 (Hoekloos, 2.8) were dosed by background dosing at 2×10^{-7} mbar while cooling down the sample from 500 to 120 K. This produced a full monolayer of H_{ad} or D_{ad}. When dosing D_2, all filaments were switched off to minimize contamination of H-atoms on the surface. All reported pressures are uncorrected for ion gauge sensitivity.

During TPD experiments the sample was placed in a collinear geometry with a differentially pumped quadrupole mass spectrometer (QMS, Balzers QMS 422). The heating rate, β, was always 1 K s^{-1}. During heating mass-to-charge ratios (m/e) = 2 (H_2), 3 (HD), 4 (D_2), 18 (H_2O), 19 (HDO), and 20 (D_2O) were monitored. Experiments where only D_2 was dosed showed no signal at m/e = 2, indicating that the amount of detected D^+ at this channel is negligible. All H_2O coverages are calculated from the integrated TPD peak areas. Our exact definition of a monolayer (ML) is given in section III.

The QMS signals for H_2, HD, and D_2 were calibrated using full monolayer TPD spectra. Step and terrace peaks were treated separately by fitting two Gaussian functions to the data. Since it is not possible to obtain a full HD layer, the HD signal was calibrated dosing approximately equal amounts of H_2 and D_2 simultaneously at a total pressure of 2×10^{-7} mbar. The measured hydrogen (deuterium) fraction, $\phi_{H_2,eq}$ ($\phi_{D_2,eq}$), can be obtained by comparing the H_2 (D_2) signal to the one of a full monolayer. Assuming that H_{ad} and D_{ad} are at equilibrium at the surface and that there is no isotope effect for recombination of the atoms, the other fractions are given by:

$$\phi_{D_2,eq} = \left(1 - \sqrt{\phi_{H_2,eq}}\right)^2 \quad (2.1)$$

$$\phi_{HD,eq} = 2 - 2\sqrt{\phi_{H_2,eq}} - 2\left(1 - \sqrt{\phi_{H_2,eq}}\right)^2 \quad (2.2)$$

Since H_2O sticks to the stainless steel walls of the differentially pumped QMS chamber, the high vacuum time constant of H_2O leads to an almost stepwise increase in the baseline of our H_2O TPD spectra. A reasonable approximation for the baseline is given by

$$y = y_0 + \frac{1}{2}\Delta y\left(\tanh\left(\frac{T - T_0}{\Delta T}\right) + 1\right) \quad (2.3)$$

where Δy is the total increase in the height of the baseline, T_0 is the center of the S-curve, typically slightly before the peak maximum, and ΔT is an arbitrary parameter to smooth out the tanh. Note that the value of ΔT does not matter for the total obtained integral, though it may affect the relative intensities of smaller peaks at lower temperatures. We have verified that this baseline correction procedure does not influence the leading edges of our TPD data.

RAIRS spectra were taken at a resolution of 4 cm^{-1} using a Fourier-transform infrared (FTIR) spectrometer (Biorad FTS 175). A series of flat and parabolic gold-coated mirrors focuses the light onto the sample and finally onto an external liquid-nitrogen-cooled mercury cadmium telluride (MCT) detector. A KRS-5 wire grid polarizer is mounted on the window where the beam enters the UHV chamber to enhance the signal-to-noise ratio. The sample temperature during scans was 100 K.

III. Results

Fig. 1 shows TPD spectra of D_2 (m/e = 4) desorbing from Pt(533). For all spectra, we dosed D_2 in excess of the required amount for saturating the surface from background dosing.[22] We start dosing at $T_{cyrstal}$ = 500 K and cool the crystal consecutively to below 120 K. This procedure minimizes simultaneous H_2 adsorption from UHV residual gas. Trace (a) shows two peaks generally observed in hydrogen desorption from stepped platinum surfaces.[40] The peaks at $\sim$370 and $\sim$260 K are generally ascribed to associative desorption from (100) steps and (111) terraces respectively.[22,40] Although a saturation value of 0.9 ± 0.05 ML has been reported,[22] we cannot confirm this value here. We simply refer to the saturated surface by θ_D = 1, without implying a D_{ad} : Pt ratio of 1 : 1. The ratio of terrace *versus* step desorption, as determined

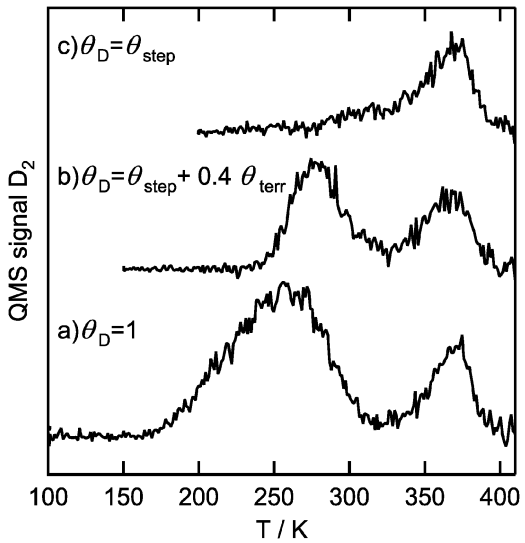

Fig. 1 TPD of D_2 after saturation dose on Pt(533) (adsorbed while cooling down from 500 to 120 K) without annealing (a), 180 s annealing at 240 K (b), and 180 s annealing at 280 K (c).

from Gaussian fits to the individual peaks at $\theta_D = 1$, yields 3 : 1. This value is strongly dependent on acceptance angle of the differentially pumped QMS, as we will discuss in a separate publication.[28] Trace (c) shows desorption of D_2 after annealing the deuterium-saturated surface for 180 s at 280 K, followed by quenching to <100 K. This extra annealing step removes nearly all deuterium required to saturate the terraces while desorption from steps remains unaltered. Trace (b) shows that annealing at lower temperatures allows for controlling the amount of removed deuterium from the (111) terraces. We have found that this procedure yields reproducible surface coverages of deuterium and minimizes contamination by simultaneous co-adsorption of H_2 from residual gas.

Fig. 2 shows TPD spectra for $m/e = 18$ and 19 after dosing various amounts of H_2O onto Pt(533) containing different deuterium pre-coverages. For clarity, we do not show the TPD spectra for $m/e = 20$, since they show the same characteristics compared to $m/e = 19$, but are much less intense. We have verified that cracking in the QMS ionizer of HOD and D_2O yields no significant contribution to the signal at $m/e = 18$ at the low signal intensities in experiments for $m/e = 19$ and 20. Therefore, the signal at $m/e = 18$ results from H_2O only within our experimental error. Similarly, the signal at $m/e = 19$ results only from HOD and the signal at $m/e = 20$ only results from D_2O. In Fig. 2a water desorbs from bare Pt(533), *i.e.* $\theta_D = 0$. In Fig. 2b, we have removed deuterium using the pre-annealing step to the extent that θ_D equals the amount required to saturate the steps, *i.e.* $\theta_D \approx \theta_{step}$. In Fig. 2c, H_2O is dosed directly after dosing a saturation coverage of deuterium, *i.e.* $\theta_D = 1$.

Detailed inspection of the TPD spectra in Fig. 2 yields the following observations. We focus first on the traces for H_2O (plotted *versus* the left axis). H_2O desorption from the bare Pt(533) surface takes place in three peaks, α_1, α_2 and α_3, with peak temperatures of ~188, ~171 and ~148 K, respectively. The peak at highest temperature, α_1, appears at the lowest H_2O coverages. At coverages <0.25 ML the peak desorption temperature shows a slight increase from 184 to 188 K with

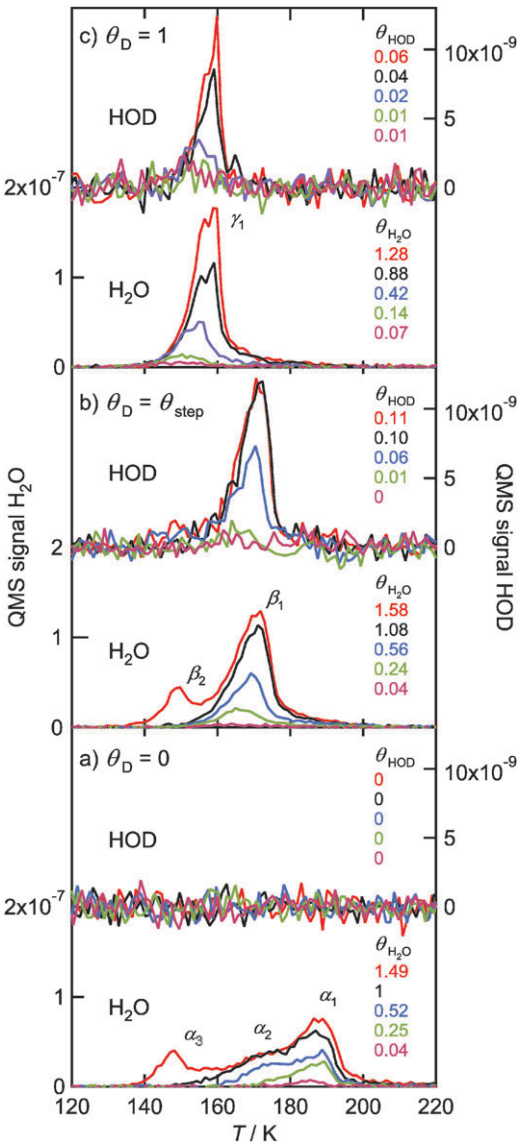

Fig. 2 TPD spectra of H_2O (left axis) and HOD (right axis) dosed on Pt(533) with $\theta_D = 0$ (a), $\theta_D = \theta_{step}$ (b), and $\theta_D = 1$ (c).

increasing dose. For $\theta_{H_2O} > 0.25$ ML, we observe no shift in desorption temperature up until saturation of the α_1 peak. The second peak, α_2, is clearly observed prior to saturation of α_1. The lowest temperature peak, α_3, is only observed when α_1 and α_2 have saturated. Following Grecea *et al.*,[9] we use the largest combined integral for α_1 and α_2 as a reference for the amount of adsorbed H_2O and refer to this amount as $\theta_{H_2O} = 1$ ML. Dosing larger quantities leads to the appearance of the α_3 peak, which has previously been shown to result from multilayer desorption.[9] When pre-adsorbing deuterium at $\theta_D = \theta_{step}$, TPD spectra for post-dosed H_2O only show two peaks, β_1 and β_2. Their peak maxima occur at 171 and 148 K for the highest H_2O coverage shown here. The β_1 peak saturates prior to the appearance of the β_2 peak. The peak desorption temperature of β_1 shifts from 164 to 171 K with increasing dose. When pre-adsorbing deuterium at $\theta_D = 1$, TPD spectra show a single peak, γ_1, initially appearing near 150 K. Desorption characteristics for this peak are typical for zero-order desorption

kinetics, *i.e.* overlapping leading edges and a peak desorption temperature that increases with dose. Interestingly, all TPD traces for $\theta_{H_2O} \geq 0.42$ ML and $\theta_D = 1$ show a splitting of the peak near the maximum desorption rate. We observe this behavior already at $\theta_{H_2O} = 0.26$ ML (not shown here).

Next, we turn to the HOD signals in Fig. 2 (plotted *vs.* right axis). Here, we first note that we are not aware of an unambiguous means to determine the integral for 1 ML HOD desorbing from the surface. Therefore, we have used the integral for 1 ML H_2O as our reference in calculating θ_{HOD}. We feel this is justified since the ionization efficiency in our QMS, the transmission through the quadrupole, and the amplification by the channeltron are not expected to vary significantly for these isotopes. Turning to the data, we observe that adsorbing H_2O on bare Pt(533) leads to no measurable desorption of HOD for any dose shown here. In contrast, HOD desorption does occur from the deuterium pre-covered surfaces in Fig. 2b and 2c. At $\theta_D = \theta_{step}$, HOD desorbs simultaneous with β_1. For the largest water post-dose we also observe a small amount of HOD desorbing simultaneous with β_2. For $\theta_D = 1$, HOD also desorbs simultaneously with H_2O in the peak labeled γ_1. Here, we also observe overlapping leading edges and a change in desorption rate in the rising part of the traces.

We have integrated all TPD spectra for the three isotopes of water (H_2O, HOD and D_2O) for varying deuterium pre-coverages. A plot of the sum of the integrated areas for these isotopes *versus* dose time indicates that the total quantity of desorbing water varies linearly with dose time. The slope of such a plot is a measure of the sticking probability. We observe that the sticking probability does not change significantly by pre-dosing any amount of deuterium, although minor changes appear comparable to our estimated experimental error. The absolute sticking probability for H_2O on Pt(533) was determined by Grecea *et al.*, and found to be 1.[9]

Fig. 3 shows TPD spectra of $m/e = 3$ (HD) and $m/e = 4$ (D_2) for different θ_D/θ_{H_2O} coverages. The signal at $m/e = 2$ (H_2) was not usable for analysis, because of the large background signal caused by objects other than the sample warming up and degassing H_2 during heating. Trace (a) was obtained after fully saturating the surface with D_{ad}, prior to adsorbing 0.94 ML H_2O. Two features are seen in both the HD and the D_2 signal: a high temperature feature at 365 K and a low temperature feature at 255 K. The high temperature feature is associated with desorption from step sites, whereas the low temperature feature is associated with desorption from terrace sites.[22] It can be clearly seen that the ratio HD_{step} : $D_{2,step}$ is much larger than the ratio $HD_{terrace}$: $D_{2,terrace}$. This shows that, at least relatively, HD is formed more on step sites than on terrace sites. Trace (b) shows HD and D_2 desorption traces when step sites are fully covered with D_{ad} and $\theta_{H_2O} = 0.46$ ML. Both the HD and D_2 signals show desorption from step sites only.

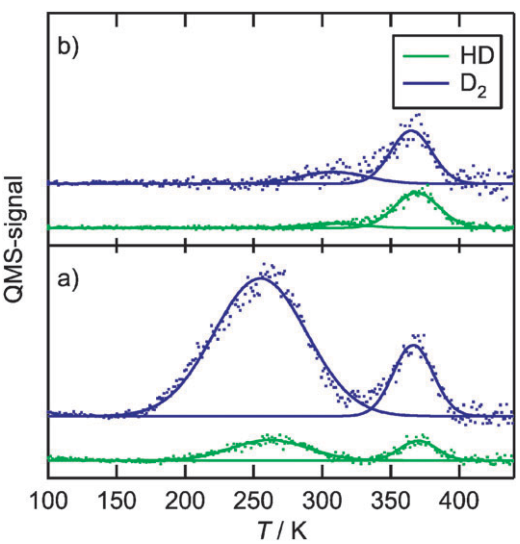

Fig. 3 TPD spectra of $m/e = 3$ (green) and 4 (blue) for (a) $\theta_D = 1$ and $\theta_{H_2O} = 0.94$ and (b) $\theta_D = \theta_{step}$ and $\theta_{H_2O} = 0.46$, both dosed on Pt(533). The solid lines show fits of two Gaussian functions to the data.

The lower panel in Fig. 4 plots the fraction of HOD and D_2O appearing in water TPD spectra for varying deuterium pre-coverages on the (111) terraces. Note that in our experiments, we must use deuterium-coverages of $\theta_D \geq \theta_{step}$, since leaving part of the steps bare results in contamination from residual H_2 in the UHV system. For both HOD and D_2O, we observe in Fig. 4 that their appearance is strongly dependent

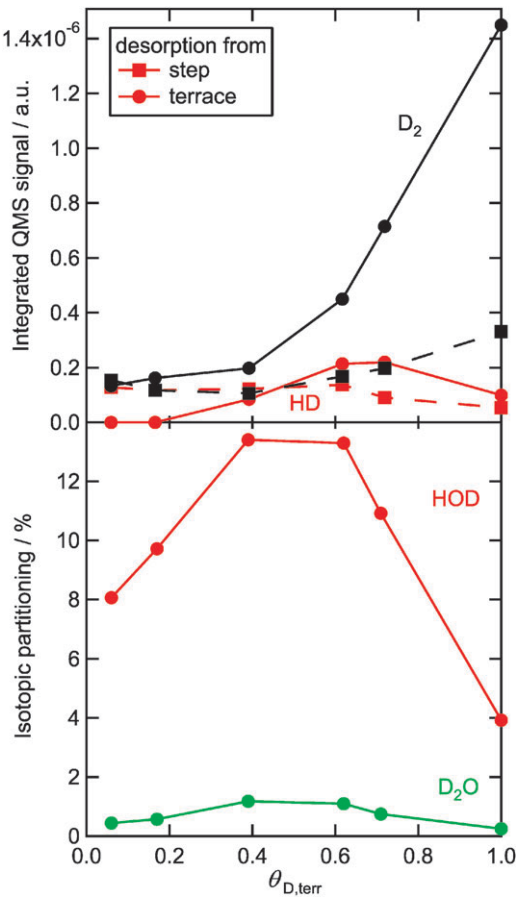

Fig. 4 Isotopic partitioning in water TPD spectra for a range of deuterium coverages on the (111) terraces of Pt(533) (lower half of frame) and the absolute amounts of subsequently desorbing HD and D_2, separated into step and terrace contributions (upper part of frame).

on the fractional deuterium pre-coverage of the (111) terraces. Production of the deuterated species peaks when terraces are approximately half covered with deuterium. The upper panel in Fig. 4 shows the absolute amounts of HD and D_2 desorbing from the surface. Step (squares and dashed line) and terrace (circles and solid line) contributions are indicated separately. We observe a maximum in the amount of HD adsorbing from terrace sites at $\theta_{D,terr} \approx 0.65$ whereas the amount of D_2 desorbing from terrace sites increases continuously with increasing $\theta_{D,terr}$. The amounts of HD and D_2 desorbing from step sites only vary significantly when θ_D is close to unity. The total water desorption varied slightly in these experiments ($0.94 < \theta_{H_2O} < 1.3$ ML). We have normalized the results in Fig. 4 for this slight variation.

The lower part of Fig. 5a shows the dependence of the isotopic partitioning for varying amounts of water dosed after creating a deuterium coverage of $\theta_D = \theta_{step}$. The lower part of Fig. 5b shows same dependence for $\theta_D = 1$. The insets show the absolute signals. For the step-covered deuterium surface we observe maximum partitioning of deuterated isotopes for $\theta_{H_2O} \sim 0.6$, although the dependence on water coverage is less pronounced than the dependence on the deuterium coverage (Fig. 4). For $\theta_{H_2O} \geq 1.2$ ML, the absolute HOD signal starts to level off. For the saturated deuterium surface, the relative yield of deuterated water is slightly higher for $\theta_{H_2O} < 1$ ML than for $\theta_{H_2O} > 1$ ML. The absolute amount of desorbing HOD increases linearly with θ_{H_2O}. The upper parts of Fig. 5a and b show the isotopic partitioning of desorbing HD. Here, we are able to determine the partitioning without use of the H_2 signal, since we have determined the absolute value of maximum integral for HD desorbing from step and terrace sites (see section II). For $\theta_D = \theta_{step}$ the fraction of desorbing HD initially increases linearly. When θ_{H_2O} becomes larger than $\sim$1.2 ML the fraction of desorbing HD starts to level off. On the D-saturated surface the fraction of HD formed on terrace sites keeps increasing linearly with H_2O dose. On step sites it levels off at $\theta_{H_2O} > 0.3$ ML. The fractional isotopic exchange is consistently larger at step sites that at terrace sites.

The inset of Fig. 6 shows the TPD spectra for water with varying deuterium pre-coverages. Here, the TPD signals are the summed signals for m/e = 18, 19 and 20. The total water coverage varies only slightly between 0.94 and 1.3 ML, whereas the deuterium pre-coverage ranges from 0 to 1. Noteworthy is the complete disappearance of the α_1 peak at 188 K upon pre-adsorption of deuterium at the coverage required to saturate the steps. For $\theta_D > \theta_{step}$, we observe that the temperature of the desorption peak maximum lowers. In Fig. 6, we show the temperature of maximum desorption rate as a function of terrace occupancy. Also, we note that in the inset of Fig. 6, the splitting of the desorption feature appears only at the highest deuterium pre-coverage. We start observing this behavior from $\theta_{D,terr} > 0.70$ onward (not shown here).

The upper line in Fig. 7a shows the RAIRS spectrum of 1 ML H_2O adsorbed on the bare Pt(533) surface. The spectrum shows two features at 3384 and at 3684 cm^{-1}. The feature at 3384 cm^{-1} is associated with the OH stretching (νOH) mode of hydrogen-bonded H_2O, whereas the (weak) feature at 3684 cm^{-1} is associated with the stretching mode of free OH-groups (*i.e.* non-hydrogen-bonded, dangling O–H

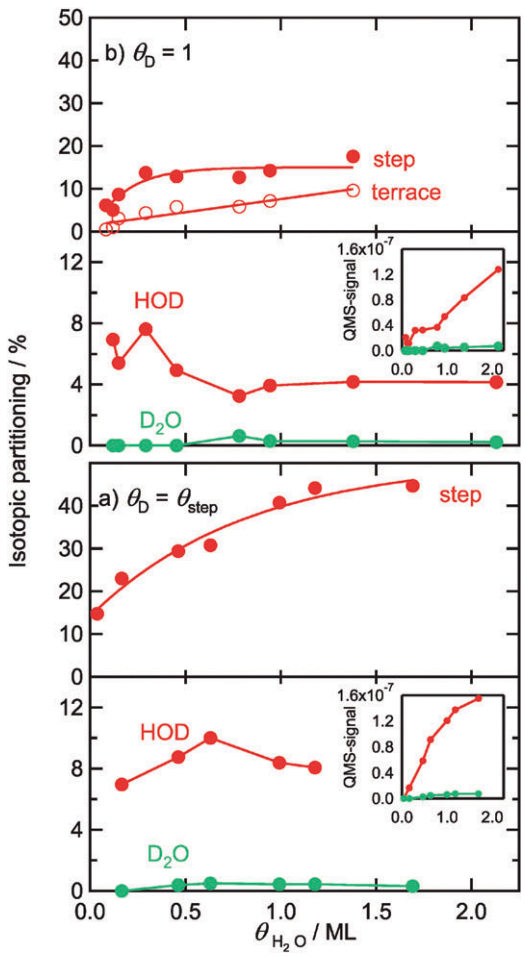

Fig. 5 Isotopic partitioning for varying water coverages on Pt(533) with (a) $\theta_D = \theta_{step}$ and (b) $\theta_D = 1$. The lower parts of the frame show the HOD (D_2O) fractions (insets show absolute amounts). The upper parts show the HD fractions, deconvoluted into terrace and step contributions. The lines are only a guide for the eye.

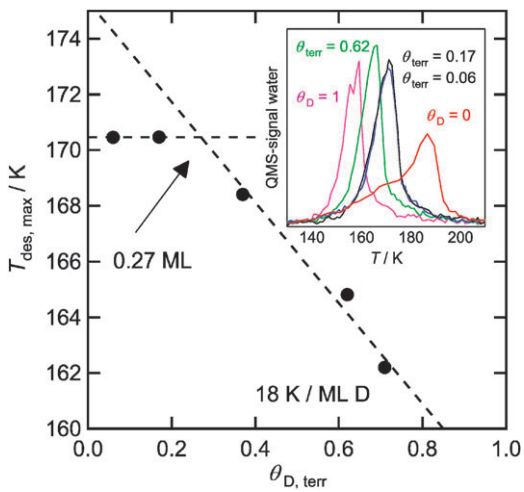

Fig. 6 Temperature of maximum desorption rate for varying deuterium pre-coverages of the Pt533 (111) terraces when $\sim$1 ML water is adsorbed. The inset shows the corresponding original TPD spectra.

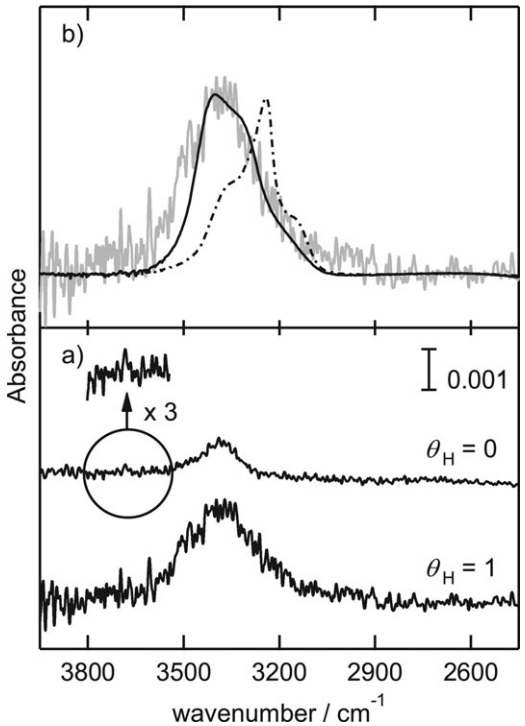

Fig. 7 (a) RAIRS spectra of ~1 ML H_2O adsorbed on Pt(533) where $\theta_H = 0$ (upper line) and $\theta_H = 1$ (lower line). (b) Comparison of RAIRS spectrum where 1 ML H_2O is adsorbed on a fully hydrogen-covered Pt(533) surface (grey line) to 45 ML ASW (solid black line) and 45 ML CI (dash-dotted line) on Pt(533).[45] The spectra for 45 ML H_2O have been divided by 100.

bonds.[41,42] The lower line shows the spectrum of 1.08 ML H_2O adsorbed on a surface pre-covered with hydrogen ($\theta_H = 1$). The feature at 3383 cm^{-1} is broader, more intense, and has become more asymmetric than for the bare surface. A small shoulder starts to appear at ~3500 cm^{-1}. The peak assigned to free OH-groups is not observed as clearly as on the bare surface. We note that when H_2 and H_2O are co-adsorbed no feature around 1150 cm^{-1} is observed on Pt(533). This is in contrast to observations on Pt(111).[29,30,33]

IV. Discussion

In this section we will discuss both adsorption and reactivity of H_2O on the (partially) deuterium-covered Pt(533) surface. We will move from adsorption on to reactivity and finally argue that they are related. However, first we address deuterium adsorption without co-adsorbing water.

The procedure used to create partially deuterium-covered surfaces leaves in all of our experiments an amount of deuterium on the surface that is at least equal to the amount required to saturate the steps. This does not *a priori* mean that all step sites are also occupied when subsequently dosing water at ~100 K. Partitioning of deuterium between terrace and steps sites could take place, leaving part of the steps unoccupied. However, recent DFT calculations for an accurate potential-energy surface (PES) for hydrogen dissociation on Pt(211) indicate that the binding energy of a hydrogen atom at step sites is ~0.35 eV larger than at any terrace site.[25] Olsen *et al.* find that adsorption of hydrogen at steps remains energetically more favorable than adsorption on all considered terrace sites up to saturation of the top edge of the (100) steps. At saturation of step sites, the $H:Pt_{step}$ ratio is 1 : 1. Furthermore, an additional barrier of 0.1 eV compared to diffusion along the terrace is found for diffusion from a step site onto the terrace, especially in the downward direction ("across the step"). Experiments probing diffusion on stepped platinum surfaces have also found that for the miscut required to create the (533) surface diffusion perpendicular to the surface is hampered relative to diffusion across the (111) terrace.[27] Preliminary experiments performed in our lab that probe exchange between hydrogen and deuterium separately adsorbed onto step and terrace sites indicate that exchange between steps and terraces is limited for partially and fully saturated surfaces. We therefore believe that in our experiments, pre-dosed deuterium saturates the (100) steps (almost) completely with any additional deuterium residing on (111) terraces when we start co-adsorbing H_2O.

Our TPD results for desorption of water from the bare Pt(533) surface are very similar to previously published results.[8,9] For example, compared to results from Grecea *et al.* we find accurate agreement regarding the 4 K increase in the α_1 peak desorption temperature for increasing dosages at low H_2O coverages. This increase is likely related to the initiation of molecular chain growth of water molecules along the step edges, as shown in STM studies of imperfect Pt(111) surfaces.[6] We also observe the appearance of the α_2 peak prior to saturation of the α_1 peak. We interpret this observation as proof of limited mobility of H_2O molecules adsorbed onto this surface. A third agreement is the saturation of α_1 and α_2 combined prior to appearance of α_3. This indicates that the water layer wets the entire surface prior to formation of a water multilayer. The same observation has been made for monolayer growth of ASW on Pt(111) using adsorption and desorption of a noble gas.[4]

In contrast to these similarities, we observe a significant discrepancy in the absolute temperatures reported for desorption peaks. For α_1, Grecea *et al.* report 198 K at a TPD rate of 2 K s^{-1} whereas we find 188 K at 1 K s^{-1}. For α_2, they report 185 K whereas we find 171 K. For the shifting peak temperature of α_3, they report an initial value of 160 K whereas we find a value of ~150 K. Both α_1 and α_2 show first-order kinetics, which causes the peak temperature to change with heating rate. We have repeated our experiments with a heating rate of 2 K s^{-1}. In this case we find 192 K for α_1 and 176 K for α_2. The difference in peak temperature caused by the heating rate is not large enough to explain the discrepancy between the data. Since the off-set seems reasonably constant, we do not expect it to result from impurities or other surface-related origins that would affect mono- and multilayer adsorption differently. Instead, we believe that it is only a matter of accuracy in determining the absolute temperature that causes the difference. Therefore, we also agree that the α_1 peak results from water molecules desorbing from (100) step sites, which provide stronger binding than terrace sites, as was supported by DFT calculations.[9] However, in contrast to the conclusion by Grecea *et al.*, we do not consider the higher temperature of α_2 when compared to desorption from the (111) plane to justify a claim of additional stabilization of water molecules

adsorbed onto (111) terraces. The desorption temperature of the α_2 peak in our studies actually agrees very well with a recent desorption study of D/D_2O from Pt(111) by Petrik and Kimmel.[31] Here, desorption from the bare (111) plane is observed at $\sim$171 K, which is the same temperature we find for α_2 and β_1. Also, our initial value for α_3 corresponds very well to the value reported for multilayer desorption from Pt(111)[31,11] and Pt(533)[8] in several recent TPD studies using low heating rates. We therefore believe that the determination of the absolute temperature by Grecea *et al*. is off-set by 6–9 K, causing an erroneous argument regarding the stabilizing effect of (100) steps on desorption from (111) terraces.

Apparently in contradiction with the previous statement, we do agree that binding of H_2O on (111) terraces is strengthened by (100) steps. However, we base our argument not on the desorption temperature of the α_2 peak, but on the quantity desorbing in α_1 and α_2. Considering the size of terraces, one may expect a ratio of H_2O bound at step sites *versus* terrace sites of the order of 1 : 3 or 1 : 4. The ratio of α_1 to α_2 should reflect this. We notice, in agreement with results reported by Grecea *et al*., that the ratio is reversed. The higher temperature peak is considerably larger than the lower temperature peak. This indicates that sites which bind water more strongly than the (111) plane are much more abundant on the [4(111) $\times$ (100)] surface than would be expected from geometrical arguments. Considering the results from DFT calculations published for this system,[9] it seems likely that molecules desorbing in the α_1 peak originate from both the upper and lower side of the (100) step, and probably also at least in part from the (111) terrace. The DFT study indicates that such locations bind water much more strongly than locations in the middle of the terrace and sites closer to the top side of the step edge. An STM study also indicates water adsorption on both sides of the step edge.[6] Therefore, we agree with Grecea *et al*. that the (100) steps strengthen binding at (111) terraces on Pt(533) but base our argument on relative quantities rather than on desorption temperatures. Terrace sites further away from step sites are unaffected. H_2O molecules desorbing from the latter sites give rise to the α_2 peak.

Adsorption of deuterium drastically alters TPD spectra for this stepped surface. The observed stabilization of water on the bare Pt(533) surface is removed entirely when pre-adsorbing deuterium at the steps (Fig. 2b). The same observation was reported when steps were covered with CO prior to adsorbing water.[9] We have repeated those experiments with CO and find the same results (not shown here). In both cases, we observe that water desorption strongly resembles desorption from the bare Pt(111) plane at 171 K. The increase in the β_1 peak desorption temperature with increasing water coverage in the range $0 < \theta_{H_2O} < 1$ ML is also observed on both Pt(111) and D_{step}/Pt(533). A difference between our spectra and those taken for the (111) surface occurs in the leading edges of the desorption traces. For Pt(111) these coincide, whereas for D_{step}/Pt(533) they do not overlap. For Pt(111), the apparent zero-order desorption kinetics have been interpreted as a result of a coexistence of a condensed water phase with a 2-dimensional gas at equilibrium.[11] Large patches of a condensed phase have been observed at lower surface temperatures by STM on broad (111) terraces.[6] The difference we observe in the leading edges suggests that, on Pt(533), the (100) steps inhibit coexistence of such a two-phase system at equilibrium. We note that the first layer of water on Pt(533) does wet the surface, though. The β_2 peak only appears when β_1 has saturated. It is also noteworthy that an equivalent of 1 ML H_2O interacts with the surface, since the integral of β_1 equals that of the sum of α_1 and α_2. This is not surprising when noting that DFT calculations indicate that hydrogen atoms at steps sites adsorb on the outer edge of the step.[25] Therefore, saturating the (100) steps with deuterium does not block adsorption sites for water, but does alter the binding energy. For CO adsorption on steps, Grecea *et al*. conclude that CO sterically blocks water from the stronger binding sites. Our results imply that deuterium does not sterically block water adsorption, but causes destabilization through an electronic effect.

For the deuterium-saturated surface, additional destabilization is observed (Fig. 2c). Water desorbs from D_{max}/Pt(533) in a single peak that shows, well below $\theta_{H_2O} = 1$ ML, multilayer desorption characteristics. The desorption temperature of γ_1 equals that of multilayer desorption from Pt(111) and the observed overlapping leading edges imply zero-order desorption kinetics. We recently found the same behavior for water desorbing from deuterium-saturated Ni(111)[43] and implied that it was due to hydrophobicity of the surface. The same appears to be the case here. If the deuterium-covered Pt(533) surface is hydrophobic, water will form 3-dimensional structures at coverages well below $\theta_{H_2O} = 1$ ML. When large enough, these 3-dimensional, multilayered structures will show zero-order desorption kinetics with a peak temperature equal to that of water desorbing from flat ASW multilayers.

Our RAIRS spectra support this structural difference between 1 ML H_2O on bare and deuterium-covered Pt(533). Fig. 7a clearly shows that upon pre-dosing hydrogen, the hydrogen-bonded OH stretch absorption near 3400 cm^{-1} broadens significantly. Increased disorder causes such broadening.[44] In Fig. 7b we compare the RAIRS spectrum of 1 ML H_2O adsorbed on the fully hydrogen-covered Pt(533) surface to RAIRS spectra for bulk (45 ML) ASW and crystalline ice (CI) on Pt(533) published by Backus *et al*.[45] Our spectrum closely resembles the spectrum they obtained for 45 ML ASW. This shows that indeed ASW is formed at coverages of only 1 ML H_2O.

An additional observation supports our claim for 3-dimensional ASW water growth on the deuterium-covered surface. We noticed in Fig. 2c a slight, but consistent change in desorption rate at the leading edge of the γ_1 peak at $\theta_D > 0.7\theta_{max}$, which leads to a double-peak structure. Such a deflection in TPD spectra was previously observed when growing ASW layers on, amongst other substrates, Pt(111).[46,47] The deflection has been shown to result from a phase change of ASW to CI during the temperature ramp. For 25 bilayers of ASW deposited on Pt(111) at 22 K, the crystallization occurs at $\sim$158 K.[11,46] We observe the deflection in our TPD spectra for, what we claim are, multilayer 3-dimensional ASW clusters at exactly the same temperature. Therefore, not only do we believe that deuterium-covered Pt(533) is hydrophobic and results in growth of ASW "snowballs", we observe the phase change in these "snowballs" to crystalline ice.

The shift in the β_1 peak desorption temperature for $\theta_{step} < \theta_D < \theta_{max}$ observed in Fig. 6 indicates a gradually decreasing binding energy for water with increasing concentration of deuterium on (111) terraces. Interestingly, Petrik and Kimmel observed a significant stabilization of water adsorbed on the Pt(111) surface with increasing deuterium coverages up to ~0.25 ML.[31] Their TPD spectra show a distinct peak at ~176 K that appears at the (almost entire) expense of the 171 K peak. The (111) terraces on Pt(533) do not reproduce this behavior for $\theta_{H_2O} \sim 1$ ML. Adsorption of deuterium on to approximately 1/4 of all terrace sites does not result in any significant change in water TPD spectra. Beyond this deuterium coverage, the peak temperature gradually shifts at a rate of approximately 18 K ML^{-1} pre-adsorbed deuterium. For Ni(111), we have observed similar behavior but with a drop in peak desorption temperature of 25 K ML^{-1}.[48] On Ni(111), where hydrogen atoms cluster to form islands, it was speculated that it results from a decreasing $(D_2O)_x$ cluster size above a certain deuterium coverage that leaves no space for ring-shaped water hexamers to adsorb on bare patches of the Ni(111) surface. For Pt(533), the same phenomenon explains our observations. The 4-atom wide terrace is large enough to support ring-shaped water hexamer structures in contact with bare platinum. DFT calculations indicate that hydrogen atoms primarily adsorb at and near step sites on platinum.[25] However, when those sites are occupied, additional deuterium must adsorb onto terrace sites further removed from the step, thereby reducing the remaining size of bare (111) patches. If deuterium interferes with formation of hexamer rings from post-dosed water, increasing concentrations of deuterium may result in formation of shorter or more branched water chains. Such structures have fewer hydrogen bonds per water molecule with decreasing cluster or chain size and are therefore stabilized less by the hydrogen-bond network. Apparently, this process is gradual and results in the gradual decrease in peak desorption temperature as observed in our TPD spectra. Although this argument, based on a steric effect between D_{ad} and H_2O, may explain our observations, we do not exclude that an electronic effect could also lie at the origin of our observations. Amongst others, STM imaging and DFT calculations may provide better understanding.

Our TPD spectra of both $m/e = 3$ and 4 and $m/e = 19$ and 20 indicate that the Pt(533) surface induces thermo-neutral exchange between H from H_2O and D_{ad}.

$$H_2O + D_{ad} \rightarrow HOD + H_{ad} \qquad (4.4)$$

Such exchange has also been observed and studied on Pt(111)[30] and Pt(100)[32] surfaces. For Pt(533), Fig. 4 and 5 show that this exchange reaction is dependent on the amounts of water and deuterium present. We observe that the exchange peaks when deuterium atoms saturate the (100) steps and cover half of the (111) terraces. The kinetics therefore seem dependent on a $\theta_{D,terr}(1 - \theta_{D,terr})$ term. This suggests that the rate of reaction improves when at least some of the post-dosed H_2O interacts directly with bare platinum atoms in the (111) terrace. However, formation of HD and HOD is not shut down when the surface is fully covered with D_{ad} and we can conclude that reaction occurs both in a mixed deuterium–water phase in contact with the metal and in a system where water is adsorbed as a multilayered structure on top of the hydrophobic deuterium-covered surface, though exchange would be faster in the former one.

For the latter case, it is instructive to consider the exact dependencies observed. For the deuterium-saturated surface we observe that HOD formation is linear up to 2 ML of water desorbing from the surface (inset in Fig. 5b). For the step-saturated surface, we observe curvature in the HOD formation already at $\theta_{H_2O} = 1.2$ ML (inset Fig. 5a). This strongly suggests that in the latter case, the total amount of D on the surface has been depleted significantly. The same figures also illustrate that multilayers of water simply act as a buffer for deuterium atoms originating at the surface. Once deuterium atoms have been exchanged at the metal surface, they quickly move into the multilayer regime through exchange:

$$H_2O + HOD \rightarrow HOD + H_2O \qquad (4.5)$$

This exchange has been studied for thicker ASW layers and was found to be very rapid.[49] Also for Pt(100) exchange as in eqn (4.5) was shown to be rapid in comparison to exchange as in eqn (4.4).[32] The quick exchange of D between water molecules causes the isotopic fraction of HOD in multilayers to reach a constant value with increasing water coverage when enough deuterium is present at the start, *i.e.* at $\theta_D = \theta_{max}$. For significantly lower starting surface concentrations (*e.g.* $\theta_D = \theta_{step}$), D_{ad} is depleted to an extent that, with increasing water coverage, the HOD and D_2O partitioning drops at higher H_2O doses.

Finally, we turn to the observed differences in the ratio for step and terrace desorption for HD and D_2. Fig. 4 shows that post-adsorption of 1 ML H_2O only yields HD desorption from steps when the initial deuterium coverage on terraces is (close to) zero. Logically, if deuterium is only present at steps, exchange can only occur there. This observation actually also strengthens our belief that atomically bound hydrogen (deuterium) at steps does not significantly diffuse to terraces in any of our experiments. As noticed before, when increasing the terrace deuterium coverage, both HD and HOD production go up and clearly peak for terrace desorption when terraces are approximately half-filled with D_{ad}. Exchange at steps sites is not affected much by the terrace deuterium concentration, as can be concluded from the absence of a significant change in HD desorption from steps. On the other hand, D_2 desorption from terraces is found to increase rapidly with increasing deuterium pre-coverage. Desorption of D_2 from steps is significantly less affected when increasing deuterium pre-coverage. These observations seem contradictory, since with more deuterium present on terraces, exchange at the terraces would be expected to become more dominant. Fig. 5b quantifies this behavior for increasing H_2O post-dose with $\theta_D = \theta_{max}$. Isotopic exchange occurs consistently almost twice as much on steps as compared to terraces.

The key to understanding this apparent contradiction lies in the connection between structure and reactivity. As we argued earlier, increasing the deuterium surface concentration on terraces induces hydrophobicity of the surface and 3-dimensional ASW growth. We believe that these "snowballs" are preferentially

located at steps, because, if they do, this would explain the bias of the exchange reaction at steps. With increasing deuterium pre-coverage on terraces, reactivity initially increases as long as D_{ad} and H_2O can co-exist on terraces and both are in contact with the metal surface. However, when the terrace deuterium coverage is high enough, water molecules are repelled toward steps, initiating 3-dimensional ASW growth. For the terraces, this lowers HD formation and increases D_2 formation. Since exchange now primarily occurs at and near steps, the total exchange drops.

From our results we can not conclude *via* which mechanism, or intermediate species, hydrogen exchange takes place. Literature suggests the formation of an hydronium-type species.[30,34] Based on our results, we can neither confirm nor disprove this claim. More detailed spectroscopic studies and DFT calculations may provide more insight in this matter.

V. Conclusion

We have observed various effects on the interaction of Pt(533) with water when deuterium is pre-adsorbed. First, the preference of deuterium to adsorb at step edges nulls the stabilization of water at steps through an electronic effect. Deuterium atoms at step edges do not block adsorption sites for water and water still wets the entire (111) terrace. However, co-existence of water as both a condensed phase and a 2-dimensional gas phase does not occur as it does on larger (111) terraces. Formation of smaller, less ordered water structures seems to replace formation of hexamer ring structures with increasing deuterium coverage. Near deuterium saturation, water preferentially forms 3-dimensional ASW clusters at the steps. These ASW clusters are large enough at an equivalent amount of less than 1 ML to allow for observation of its phase transition to crystalline ice. Although exchange of D_{ad} with H_2O occurs both at steps and terraces and is dependent on both surface coverages, the preference of water molecules to cluster at the step sites on the hydrophobic, deuterium-saturated Pt(533) surface biases exchange toward steps.

Acknowledgements

We kindly thank Prof. Aart W. Kleyn and FOM for use of equipment. We also thank Ellen Backus for making available the infrared data on bulk water on Pt(533). This work was supported financially by the Netherlands Organization for Scientific Research (NWO).

References

1 P. A. Thiel and T. E. Madey, *Surf. Sci. Rep.*, 1987, **7**(6–8), 211–385.
2 M. A. Henderson, *Surf. Sci. Rep.*, 2002, **46**(1–8), 1–308.
3 G. Zimbitas and A. Hodgson, *Chem. Phys. Lett.*, 2006, **417**(1–3), 1–5.
4 G. A. Kimmel, N. G. Petrik, Z. Dohnálek and B. D. Kay, *J. Chem. Phys.*, 2006, **125**(4), 044713.
5 G. Zimbitas, S. Haq and A. Hodgson, *J. Chem. Phys.*, 2005, **123**(17), 174701.
6 M. Morgenstern, T. Michely and G. Comsa, *Phys. Rev. Lett.*, 1996, **77**(4), 703–706.
7 H. Ogasawara, J. Yoshinobu and M. Kawai, *J. Chem. Phys.*, 1999, **111**(15), 7003–7009.
8 D. C. Skelton, R. G. Tobin, G. B. Fisher, D. K. Lambert and C. L. DiMaggio, *J. Phys. Chem. B*, 2000, **104**(3), 548–553.
9 M. L. Grecea, E. H. G. Backus, B. Riedmüller, A. Eichler, A. W. Kleyn and M. Bonn, *J. Phys. Chem. B*, 2004, **108**(33), 12575–12582.
10 K. Jacobi, K. Bedürftig, Y. Wang and G. Ertl, *Surf. Sci.*, 2001, **472**(1–2), 9–20.
11 J. L. Daschbach, B. M. Peden, R. S. Smith and B. D. Kay, *J. Chem. Phys.*, 2004, **120**(3), 1516–1523.
12 G. B. Fisher and J. L. Gland, *Surf. Sci.*, 1980, **94**(2–3), 446–455.
13 X. Su, L. Lianos, Y. R. Shen and G. A. Somorjai, *Phys. Rev. Lett.*, 1998, **80**(7), 1533–1536.
14 R. S. Smith, C. Huang, E. K. L. Wong and B. D. Kay, *Phys. Rev. Lett.*, 1997, **79**(5), 909–912.
15 K. Christmann, G. Ertl and T. Pignet, *Surf. Sci.*, 1976, **54**, 365–392.
16 Ş. C. Bădescu, P. Salo, T. Ala-Nissila, S. C. Ying, K. Jacobi, Y. Wang, K. Bedürftig and G. Ertl, *Phys. Rev. Lett.*, 2002, **88**(13), 136101.
17 Ş. C. Bădescu, K. Jacobi, Y. Wang, K. Bedürftig, G. Ertl, P. Salo, T. Ala-Nissila and S. C. Ying, *Phys. Rev. B*, 2003, **68**(20), 205401.
18 S. L. Bernasek and G. A. Somorjai, *J. Chem. Phys.*, 1975, **62**(8), 3149–3161.
19 M. Salmeron, R. J. Gale and G. A. Somorjai, *J. Chem. Phys.*, 1977, **67**(11), 5324–5334.
20 A. M. Baró and H. Ibach, *Surf. Sci.*, 1980, **92**(1), 237–246.
21 T. H. Lin and G. A. Somorjai, *J. Chem. Phys.*, 1984, **81**(2), 704–709.
22 A. T. Gee, B. E. Hayden, C. Mormiche and T. S. Nunney, *J. Chem. Phys.*, 2000, **112**(17), 7660–7668.
23 D. A. McCormack, R. A. Olsen and E. J. Baerends, *J. Chem. Phys.*, 2005, **122**(19), 194708.
24 A. M. Baró, H. Ibach and H. D. Bruchmann, *Surf. Sci.*, 1979, **88**(2–3), 384–398.
25 R. A. Olsen, S. C. Badescu, S. C. Ying and E. J. Baerends, *J. Chem. Phys.*, 2004, **120**(24), 11852–11863.
26 A. P. Graham, A. Menzel and J. P. Toennies, *J. Chem. Phys.*, 1999, **111**(4), 1676–1685.
27 C. Z. Zheng, C. K. Yeung, M. M. T. Loy and X. Xiao, *Phys. Rev. B*, 2004, **70**(20), 205402.
28 I. M. N. Groot, K. J. P. Schouten, O. T. Berg, A. W. Kleyn and L. B. F. Juurlink, in preparation.
29 F. T. Wagner and T. E. Moylan, *Surf. Sci.*, 1988, **206**(1–2), 187–202.
30 D. Lackey, J. Schott, J. K. Sass, S. I. Woo and F. T. Wagner, *Chem. Phys. Lett.*, 1991, **184**(4), 277–281.
31 N. G. Petrik and G. A. Kimmel, *J. Chem. Phys.*, 2004, **121**(8), 3727–3735.
32 N. Kizhakevariam and E. M. Stuve, *Surf. Sci.*, 1992, **275**(3), 223–236.
33 Y. Shingaya and M. Ito, *Surf. Sci.*, 1996, **368**(1–3), 318–323.
34 N. Chen, P. Blowers and R. I. Masel, *Surf. Sci.*, 1999, **419**(2–3), 150–157.
35 M. J. Iedema, M. J. Dresser, D. L. Doering, J. B. Rowland, W. P. Hess, A. A. Tsekouras and J. P. Cowin, *J. Phys. Chem. B*, 1998, **102**(46), 9203–9214.
36 M. Osawa, M. Tsushima, H. Mogami, G. Samjeské and A. Yamakata, *J. Phys. Chem. C*, 2008, **112**(11), 4248–4256.
37 E. Skúlason, G. S. Karlberg, J. Rossmeisl, T. Bligaard, J. Greeley, H. Jónsson and J. K. Nørskov, *Phys. Chem. Chem. Phys.*, 2007, **9**(25), 3241–3250.
38 H. G. Jenniskens, A. Bot, P. W. F. Dorlandt, W. van Essenberg, E. van Haas and A. W. Kleyn, *Meas. Sci. Technol.*, 1997, **8**(11), 1313–1322.
39 B. Riedmüller, F. Giskes, D. Glastra van Loon, P. Lassing and A. W. Kleyn, *Meas. Sci. Technol.*, 2002, **13**(2), 141–149.
40 K. E. Lu and R. R. Rye, *Surf. Sci.*, 1974, **45**(2), 677–695.
41 B. Rowland and J. P. Devlin, *J. Chem. Phys.*, 1991, **94**(1), 812–813.
42 V. Buch and J. P. Devlin, *J. Chem. Phys.*, 1991, **94**(5), 4091–4092.
43 J. Shan, J. F. M. Aarts, A. W. Kleyn and L. B. F. Juurlink, *Phys. Chem. Chem. Phys.*, 2008, **10**(16), 2227–2232.

44 M. W. Urban, *Vibrational spectroscopy of molecules and macromolecules on surfaces*, Wiley-Interscience, New York, 1993.
45 E. H. G. Backus, M. L. Grecea, A. W. Kleyn and M. Bonn, *Phys. Rev. Lett.*, 2004, **92**(23), 236101.
46 P. Löfgren, P. Ahlström, D. V. Chakarov, J. Lausmaa and B. Kasemo, *Surf. Sci.*, 1996, **367**(1), L19–L25.
47 Z. Dohnálek, R. L. Ciolli, G. A. Kimmel, K. P. Stevenson, R. S. Smith and B. D. Kay, *J. Chem. Phys.*, 1999, **110**(12), 5489–5492.
48 J. Shan, J. F. M. Aarts, A. W. Kleyn and L. B. F. Juurlink, *Phys. Chem. Chem. Phys.*, 2008, **10**(32), 4994–5003.
49 R. S. Smith, Z. Dohnálek, G. A. Kimmel, K. P. Stevenson and B. D. Kay, *Chem. Phys.*, 2000, **258**(2–3), 291–305.